Documentation and significance of the perirheic zone on inundated floodplains

Leal A. K. Mertes

Department of Geography and Institute for Computational Earth System Science, University of California, Santa Barbara

Abstract. The transfer of water, sediment, and other materials to floodplains is a function of the hydrology of inundation. Inundation of floodplains by regional water, that is, overbank flow from the main river channel, and local water, that is, groundwater, hyporheic water, local tributary water, and direct precipitation onto the floodplain, is such that some rivers inundate dry floodplains, while other rivers inundate fully saturated floodplains. Remote sensing and field data from the large rivers Missouri, Mississippi, Amazon, Ob'-Irtysh, Taquari, and Altamaha show a variety of water types on inundated floodplains, including areas of mixing of river and local water defined as the "perirheic zone." For the rivers examined here, only the Missouri River flooded its entire valley with sediment-rich river water. Therefore the floodplains of these large rivers from the Arctic to the Amazon are only partially inundated with river water during floods and the corresponding perirheic zones may encompass a significant floodplain ecotone.

1. Introduction

Inundation of a floodplain is the result of flooding from different water sources and may occur before a river overtops its banks or levees. The components of inundation hydrology can be expressed in terms of the mass balance of water in a channel-floodplain reach (Figure 1), where the mass balance is expressed as a function of the volumetric change in storage of water in the reach (ΔS_r) with

$$\Delta S_r = \text{time} \times [Q_{in} + Q_{tr} - Q_l - Q_p + Q_{gw} - (Q_{out} + Q_e + Q_{gw})]. \quad (1)$$

Subscripted Q terms represent discharge as volume per unit time that are defined and illustrated in Figure 1. Positive terms are inputs and negative terms are outputs. The mass balance of discharges includes river water input to and output from the reach. For the scale of the rivers considered in this paper (Table 1), large tributaries contribute input from regional-scale watersheds (10^4–10^6 km^2), while small tributaries contribute input from local watersheds on the scale of the floodplain area (10^2–10^3 km^2). Water can also enter the reach via groundwater and precipitation onto the channel, floodplain, or slopes that drain directly onto the floodplain surface. Evaporation from the channel and floodplain completes the mass balance for the reach.

If the water balance for just the floodplain were considered in terms of the volumetric change in storage (ΔS_f) then the exchange terms between the river and floodplain (Q_{rf} and Q_{fr}) would need to be included according to

$$\Delta S_f = \text{time} \times [Q_l + Q_p - Q_{rf} + Q_{gw} - (Q_e + Q_{fr} + Q_{gw})]. \quad (2)$$

Water travels to and from the main river channel through channelized and diffuse subsurface and surface flows. The mixing of river water and groundwater in the subsurface occurs in an area known as the hyporheic zone [*Dahm and Valett*, 1996]. Hyporheic water can flow to or from the floodplain, thus contributing to both Q_{rf} and Q_{fr}. Surface flows from a channel to its floodplain occur during floods as nonchannelized overbank

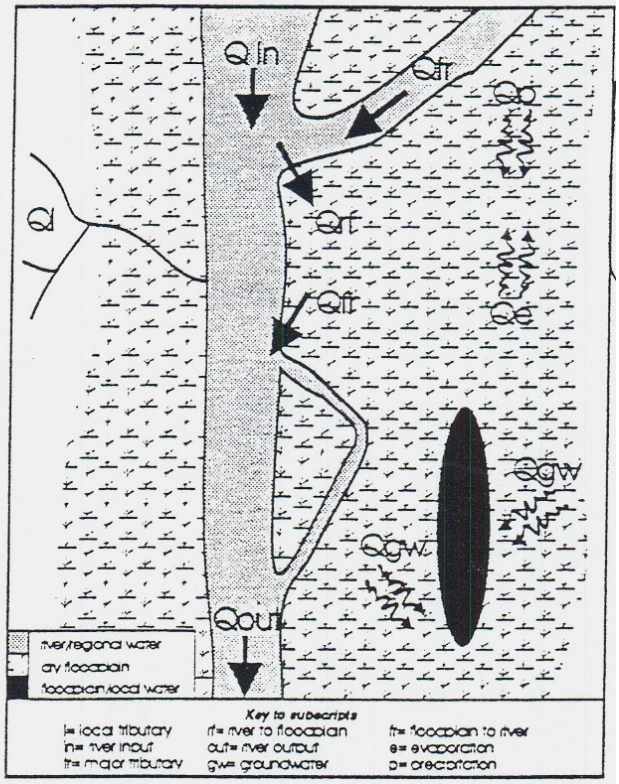

Figure 1. Components of inundation hydrology. The mass balance of discharges are represented as Q with subscripts to discriminate the components.

Paper number 97WR00658.
0043-1397/97/97WR-00658$09.00

Table 1. General Characteristics of Rivers and Remote Sensing Data for Rivers Documented in This Study

River Name (Gage Location)	Drainage Basin Area, km²	MAD,* m³ s⁻¹	Reported Flood Discharge, m³ s⁻¹	Reservoir Gross Capacity,* % of MAD	Degree of Impact*	Remote Sensing Instrument	Date of Image Acquisition	Landsat Path/Row
Missouri (Hermann, Missouri)	1,358,000	2,200†	21,200	30–35	strongly affected	Landsat TM5	July 25, 1993	25/33
Mississippi (Keokuk, Illinois)	308,000	1,800†	12,000	30–35	strongly affected	Landsat TM5	July 25, 1993	25/32
Amazon (Manacapuru, Brazil)	2,200,000‡	100,000‡	140,000‡	<5	minimally affected	Landsat TM5	Aug. 2, 1989	230/62
Ob'-Irtysh (Salekhard, Russia)	2,950,000§	12,800	29,400‖	~15	moderately affected	SPOT2 XS	July 23, 1993	61°17'N, 68°35'E¶
Taquari (Coxim, Brazil)	29,000	200–300**	no data	<5**	minimally affected	Landsat TM5	April 6, 1988	226/73
Altamaha (Doctortown, Georgia)	35,000	400	800–1000††	~8	moderately affected	Landsat TM5	Sept. 26, 1984	17/38

Locations of rivers shown in Figure 3. MAD, mean annual discharge.
*Dynesius and Nilsson [1994]. MAD estimates as the discharge prior to human impact.
†SAST [1994].
‡Richey et al. [1989].
§Bobrovitskaya et al. [1996].
‖L. Smith (unpublished data, 1993).
¶Latitude and longitude at center of image.
**O. Souza (unpublished data, 1996).
††U.S. Geological Survey [19••].

flows and flow into channels on the floodplain surface. Draining of a floodplain during recession of a flood augments Q_{fr} [*Hughes*, 1978, 1980; *Lewin and Hughes*, 1980].

The typical pattern described for movement of water between channels and their floodplains is embodied in the "flood pulse" concept expressed by *Junk et al.* [1989] and illustrated in Figure 2a. *Junk et al.* [1989] described the flood pulse as a moving littoral zone of ever-increasing inundation on the floodplain. This pattern is common when the floodplain is essentially dry before overbank flooding from the river channel occurs. As depicted in Figure 2a, when the water rises the zone of flooding expands parallel to the river as levees are overtopped along the main channel and floodplain channels. Eventually, the entire floodplain is filled with increasingly deep river water, with the possible exception of areas near local tributaries where water from the main channel might mix with water from the small tributary.

However, during floods the incursion of river water across the surface of a floodplain (Q_{rf}) may be resisted by water already present on the floodplain due to groundwater, hyporheic water, flooding of local tributaries, runoff from surrounding slopes, direct precipitation, and antecedent water from prior floods. The saturation of the floodplain through these sources may occur prior to the crest of the flood wave and the

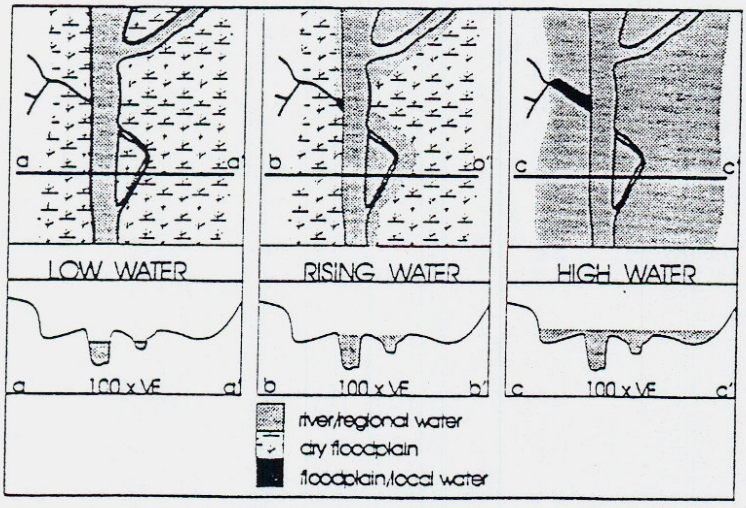

Figure 2a. Inundation pattern for a dry floodplain. The upper three graphs are planform views of a typical river, with cross sections shown in the lower three graphs with vertical exaggeration on the order of 100 times. Conditions for three water levels are illustrated, with mixing of water types shown for surface waters only. Subsurface waters are not illustrated.

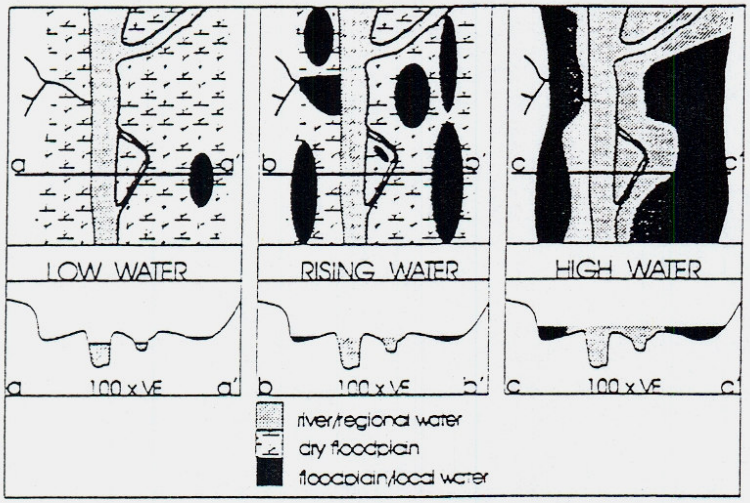

Figure 2b. Inundation pattern for a saturated floodplain. The topographic characteristics for this floodplain are generally the same as for Figure 2a. The upper three graphs are planform views of a typical river, with cross sections shown in the lower three graphs with vertical exaggeration on the order of 100 times. Conditions for three water levels are illustrated, with mixing of water types shown for surface waters only. Subsurface waters are not illustrated.

onset of overbank flooding from the river channel and may produce the pattern of flooding illustrated in Figure 2b.

The channel-floodplain system shown in Figure 2b is similar to that shown in Figure 2a, except for the presence of saturated soils or ponded water on the floodplain surface, which is perhaps due to local soil differences and recent intense rainfall. As the water rises, but does not overtop its banks, rain may continue to fall directly on the floodplain, and the floodplain would continue filling with local water. Although the river remains within its banks during the rising water period, large areas of saturated/ponded floodplain may form far from the river channel. By the time the river floods its banks, there is sufficient water on the floodplain such that the valley is only partially flooded by river water, and mixing of the water types occurs.

The mixing zone is shown as parallel bands in Figure 2b. The particular pattern of mixing of surface waters will be a function of the composition of and pressure distributions across water bodies on the floodplain. The pressure distributions vary as a function of the water balances described by (1) and (2). For example, a large floodplain lake with sufficient runoff from its local drainage basin could have sufficient head to completely prevent the entry of river water into the floodplain [*Forsberg et al.*, 1988; *Lesack and Melack*, 1995]. This type of pressure balance could produce a well-defined boundary between the river and lake water. In contrast, a more heterogeneous boundary could be produced if intense rainfall occurs on the floodplain prior to the onset of overbank flow. As a result of the rain, patches of ponded water of multiple sizes could be distributed across the floodplain (Figure 2b). Overbank flow from the river may absorb the small patches of water. At the other extreme, the large patches may be surrounded by river water and never be completely absorbed, thus producing a mixing zone that conforms approximately to the shape of the topography controlling the location of the ponding.

In this paper, patterns of mixing will be documented for reaches of six large rivers and will be shown to vary along and among these rivers. Complementary to the hyporheic zone (in the sense of *Dahm and Valett* [1996]) the mixing zone of the surface waters is defined as the "perirheic zone." This zone performs the functions of an ecotone (in the sense of *Holland* [1996]) by serving as a boundary between source waters of differing chemistry and turbidity. Variation in the spatial pattern and extent of the perirheic zone is expected to have a strong influence on the geomorphology, biogeochemistry, productivity, and vegetation of individual floodplains, and examples of these influences are discussed.

1.1. Boundaries on Floodplains

The intent of this paper is to document the existence and significance of a mixing zone of regionally derived river water with locally derived floodplain water on the surface of many inundated floodplains. To put this discussion into the context of current research on channel-floodplain systems, it is important to describe the properties of this surficial mixing zone that distinguish it from other recognized zones of mixing, most notably the hyporheic zone. Showing the significance of surficial mixing requires understanding how this zone acts as a boundary, thus enhancing the ecotonal properties of many floodplains.

Floodplains are inherently transitional between river and terrestrial systems and thus are expected to encompass many boundaries. *Naiman et al.* [1988] discussed in detail the importance of boundaries, that is, ecotones, between resource patches or ecosystems for providing stability and resiliency to the environment. According to their experience, ecotones can be effectively quantified in terms of their size, shape, resource patch dimensions, biotic composition, and contrast. Adding information on the scale and intensity of the events creating or maintaining the ecotone completes the description. By examining the frequency of ecotones normalized to resource patch size they predicted that a moderate frequency of ecotones enhances biodiversity by allowing for an optimal mix of patch and edge habitats.

An ecotone with well-described attributes is the hyporheic zone. *Dahm and Valett* [1996] summarize the historical development of current understanding of the conditions characterizing the hyporheic zone. The word was originally coined by *Orghidan* [1959] from the Greek words for flow or current ("rheo") and under ("hypo") [*Dahm and Valett*, 1996]. The critical element of the hyporheic zone is the mixing of river water with groundwater in the substrate [*Triska et al.*, 1989; *Stanford and Ward*, 1993]. The mixing may occur up to several meters below the subsurface [*Castro and Hornberger*, 1991] and several hundreds of meters laterally into the floodplain [*Stanford and Ward*, 1988]. When hyporheic flow reemerges on the floodplain in the form of "spring brooks," it adds an element to the complex of hydrologic pathways associated with the channel-floodplain system [*Stanford and Ward*, 1993]. The hyporheic zone in its lateral and longitudinal dimensions has been defined as the hyporheic corridor [*Ward and Stanford*, 1995; *Stanford and Ward*, 1988], and its extent is partially a function of the alongstream connectivity of the alluvial aquifer [*Bencala*, 1993].

The hydrologic characterization of the hyporheic zone has been aided by measurement of water chemistry and flow rates in strategically distributed wells [e.g., *Palmer*, 1993; *Triska et al.*, 1989; *Stanford and Ward*, 1988, 1993; *Dahm and Valett*, 1996] and through injection of tracers [*Castro and Hornberger*, 1991]. These types of measurements indicate that the hyporheic zone typically has several layers and can be divided according to storage times and flow rates [*Castro and Hornberger*, 1991] and percentage of stream water [*Triska et al.*, 1989; *White*, 1993]. The hydrologic and chemical gradients impart the ecotonal properties that appear to promote high diversity communities and community types in the hyporheic zone [*Valett et al.*, 1993; *Hakenkamp et al.*, 1993]. *Stanford and Ward* [1993, p. 48] suggest that it is the "dynamic convergence of aquifer-riverine components [that] adds physical heterogeneity and functional complexity to floodplain landscapes," thus enhancing biodiversity in the subsurface as suggested by the conceptual framework of *Naiman et al.* [1988].

The hyporheic corridor is fundamentally composed of "serial convergences of surface and groundwater connected by variable accumulation of porous alluvium" [*Stanford and Ward*, 1993, p. 48]. Hence a well-developed hyporheic zone is unlikely where the alluvium is fine and subsurface flow rates are low. As suggested by *Stanford and Ward* [1993] the floodplain areas with finer alluvium may have a less-active hyporheic zone. Instead, in these areas water may tend to pond more on the floodplain surface; thus there is a greater potential for mixing of flooding river water with ponded floodplain water.

The hydrology of the surface flows on inundated floodplains is often considerably more complex and includes more ecotones than as expressed by the simplest case (Figure 2a) of the moving littoral zone of the flood pulse concept [*Junk et al.*, 1989]. The complexity of inundation hydrology was generically described by *Hughes* [1978, 1980] and *Lewin and Hughes* [1980], and *Richey et al.* [1989] quantified many of the components shown in Figure 1 for the Amazon River. However, key components that have a significant influence on the patterns of mixing on inundated floodplains have not yet been fully considered. As described earlier there are at least four components that have not yet been sufficiently integrated into the framework for inundation hydrology. Hyporheic water resurfacing as spring brooks [*Stanford and Ward*, 1993] provides water that may have chemical similarities to both river and subsurface waters, but when reentering the surface flows on an inundated floodplain, it often has an entirely different level of turbidity owing to its travel through the substrate and will therefore dilute the more typically sediment-rich overbank flows from the channel. Three other components, direct precipitation on the floodplain, groundwater seepage to the surface, and local runoff directly onto the floodplain or through small tributaries (Figure 1) may lead to saturated or flooded conditions on the floodplain surface prior to flooding directly from overbank flow of the river channel. For example, *Scientific Assessment and Strategy Team* (*SAST*) [1994, p. 44] generally referred to this effect as "interior flooding" with respect to the 1993 Mississippi River floods.

The spatial and temporal variations in the relative inputs of the river water from regional sources and the local floodplain water may cause some reaches of the floodplain to be dry when overbank flows enter them (Figure 2a), while in other reaches the overbank flows may encounter fully saturated conditions (Figure 2b). The longitudinal zone resulting from surficial lateral gradients in turbidity and water chemistry includes all of the elements requisite for an ecotone in that it derives resources from multiple "homogeneous" patches and provides a temporally and spatially dynamic boundary between these resource patches. With reference to the hyporheos, I suggest that the surface zone of mixing surrounding ("peri") the flowing river water ("rheo") on inundated floodplains be named the "perirheic zone."

The hydrologic variability of the perirheic zone will be influenced by many of the same components that influence the development of the hyporheos, and will vary seasonally, laterally, and longitudinally in river corridors. One element that requires special consideration is the hydroclimatology of regional water sources versus local ones. The hydroclimatology of flooding includes consideration of the effects of the size of the cells providing precipitation for flood events [e.g., *Hayden*, 1988; *Hirschboeck*, 1988; *SAST*, 1994]. The cell size may vary from the mesoscale (defined in this paper as local) of a thunderstorm (10^2 km^2) to the synoptic scale (defined in this paper as regional) of tropical and extratropical cyclones (10^4–10^6 km^2), according to *Hirschboeck* [1988, Figure 1, p. 28]. In a large watershed the local and regional events triggering floods may be temporally out of phase or floods may be triggered by multiple local-scale events occurring rapidly in succession. The intersection of precipitation events in a given watershed will control the amount of water available from the different sources depicted in Figure 1 and (1) and (2), and therefore the amount of the different water types available for inundation of floodplains.

1.2. Study Areas

To document the existence of extensive perirheic zones on river floodplains, several reaches of large rivers around the world were studied using remote sensing data and/or field data. The locations of the rivers documented in this study, the Missouri, Mississippi, Amazon, Ob'-Irtysh, Taquari, and Altamaha, are shown in Figure 3, and their general characteristics are listed in Table 1. The size of the average discharge for the studied river reaches ranged from 400 m^3 s^{-1} to 100,000 m^3 s^{-1} with upstream drainage areas ranging from 30,000 km^2 to ~2,000,000 km^2. The degree of river management can partially be expressed by the percentage of the total annual flow stored in reservoirs, which ranges from less than 5% to over 30%. Using the criteria of *Dynesius and Nilsson* [1994] the degree of

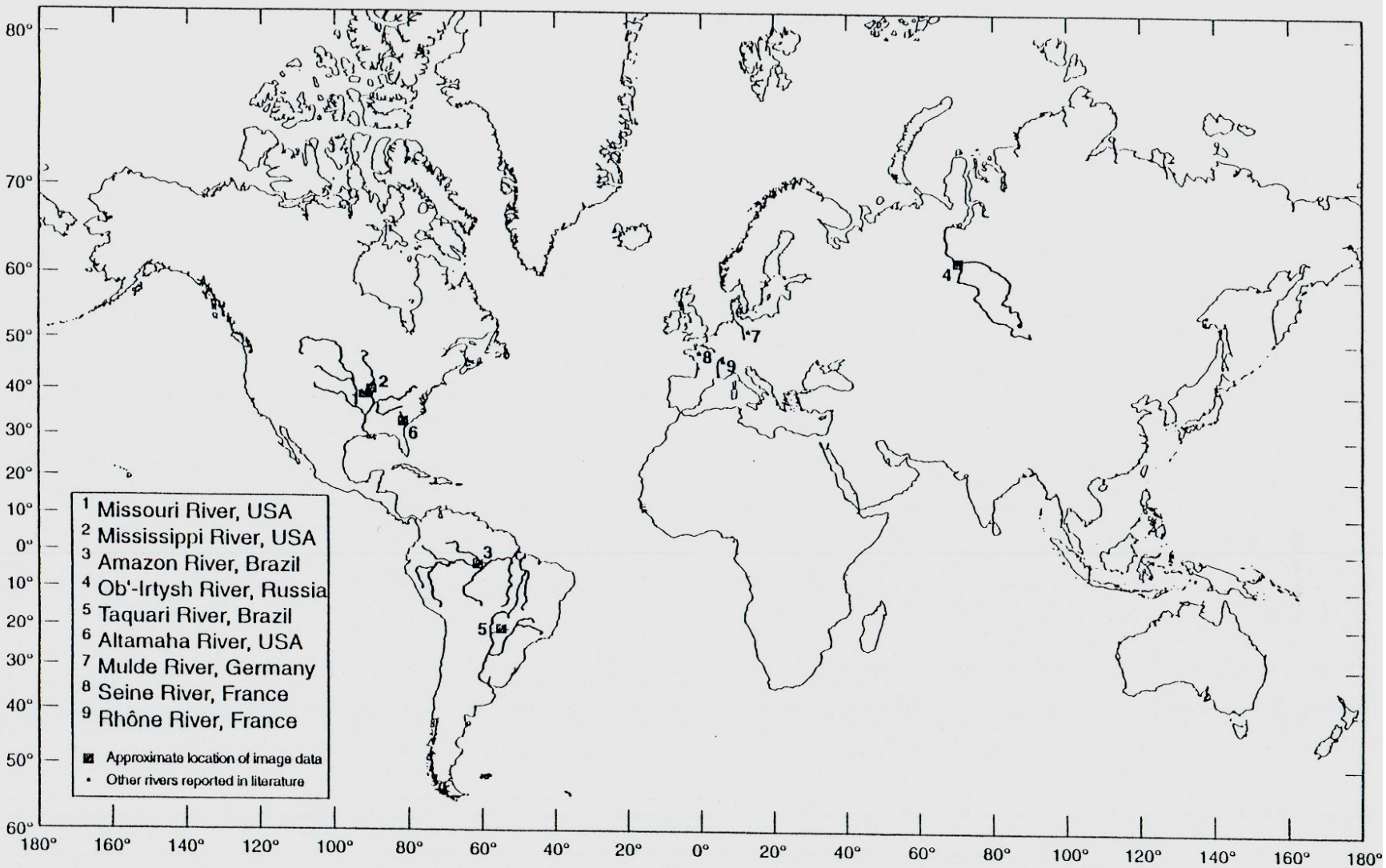

Figure 3. Location of rivers included in this study. Small shaded rectangles show approximate locations of remote sensing images displayed in Plates 1 and 2 and Figure 4. The asterisks mark the rivers for which data published by other researchers are discussed.

human impact ranges from minimally affected to strongly affected.

As previously discussed, the hydroclimatology responsible for producing floods on individual rivers will exert a strong influence on the spatial and temporal variability of the perirheic zone. The hydroclimatology of each river is summarized according to the criteria described by *Hayden* [1988]. In general, the river reaches are exposed to the extremes in climate from the cold, snowy regions of the Siberian watersheds feeding the Ob'-Irtysh to the equatorial movement of the Intertropical Convergence Zone (ITCZ) producing the Amazon floods. According to Hayden, the Ob'-Irtysh Rivers are subjected to perennially baroclinic conditions with moderate rainfall due to an inadequate supply of atmospheric moisture. Flooding is predominantly related to snowmelt in the spring. The Missouri-Mississippi system is predominantly barotropic in summer, but fronts and frontal cyclones occur. Tropical storms occasionally penetrate to the midwestern interior of the United States. The diverse sources of precipitation in the basin, including snowmelt in the spring, result in year-round flood potential. The Altamaha River, in the southwestern section of the state of Georgia, is exposed to intensely barotropic conditions in summer, but fronts and cyclones are common all year. Tropical storms and thunderstorms associated with frontal cyclones may result in heavy rains and floods in all seasons. The Taquari River, of the Pantanal wetlands in western Brazil, is exposed to perennial barotropic conditions but is also influenced by organized systems south of the ITCZ that include tropical storms. The Amazon River is perennially barotropic, with the movement of the ITCZ from north to south controlling the patterns of often intense rainfall.

2. Methods

2.1. Remote Sensing Methods and Data

It is often possible to identify the zones influenced by river water in contrast to local water because the water types may differ significantly in the quantity of suspended materials. Optical remote sensing data of a resolution fine enough to involve at least four or five pixels across the flooded area provide an opportunity to document and characterize the perirheic zone across large floodplain areas. Optical data are ideally suited for analyzing relative concentrations of suspended materials [*Dekker et al.*, 1995] because the upwelling radiance, which is the physical property measured by remote sensing detectors [*Kirk*, 1986], increases monotonically with an increase in number of particles in suspension. In addition to the scattering of light by particles, particles, dissolved materials, and the water itself absorb light. All of these effects combine to produce a nonlinear but monotonically increasing relationship between particle concentration and detected radiance.

Mertes et al. [1993] developed an application of spectral mixture analysis to estimate the concentration of suspended sediment in surface waters of the Amazon River wetlands, and it was applied in this study. Spectral mixture analysis relies on least squares techniques to decompose defined gradients in image data [*Smith et al.*, 1990; *Mertes et al.*, 1993]. The gradients, or mixing lines, are defined in terms of the spectra of selected end-members. End-members are defined as the purest representation of a material in the laboratory, in the field, or on an image. If the image can be calibrated to a surface reflectance, then absolute sediment concentration in milligrams per liter can be derived [*Mertes et al.*, 1993; *Gomez et al.*, 1995]. If the image cannot be calibrated, then relative sediment concentrations can be determined [*Mertes et al.*, 1995]. Both methods were used in this study and are described in the next section. Table 1 lists the acquisition dates for and the geographic center of the remote sensing images shown in Plates 1 and 2. All of the images were recorded during high flow conditions, when the floodplain of each river was inundated, except the Altamaha River for which a low-water image was used to delineate the channel boundary.

Images from the Amazon, Missouri, and Mississippi Rivers were all calibrated to a surface reflectance (Plate 1). The Amazon image was converted using coefficients calculated by *Mertes et al.* [1993]. The Missouri and Mississippi images were calibrated according to radiometric coefficients listed by *Markham and Barker* [1986] and estimates of path radiance from the image data. After calibration to surface reflectance, suspended sediment concentrations were estimated for each pixel using the spectral mixture analysis technique. Reference spectral end-members were based on laboratory reflectance data for sediment-water mixtures that included resuspended Mississippi River sediment [*Witte et al.*, 1981]. Reflectance end-member fractions were related to absolute sediment concentrations by a nonlinear calibration curve [*Mertes et al.*, 1993]. The estimated error is ± 20 mg L^{-1}, and results have been corroborated with field data from the Amazon [*Mertes et al.*, 1993; *Mertes*, 1994] and Mississippi channel-floodplain systems [*Gomez et al.*, 1995]. For clarity, the resulting images (Plate 1) are masked to cover unflooded areas and areas where vegetation screens the water surface.

In many cases it is not possible to accurately estimate the appropriate radiometric and atmospheric corrections to produce images of surface reflectance. Without surface reflectance data it is not possible to apply calibrations associated with laboratory spectra. For the Ob'-Irtysh, Altamaha, and Taquari Rivers it was not possible to produce surface reflectance images. Therefore, instead of relying on the laboratory end-members, image end-members for muddy and clear water were selected for the Ob'-Irtysh and Altamaha images. A vegetation image end-member was additionally selected for the Taquari River image. The result of this uncalibrated spectral mixture analysis is the production of fraction images which represent for each pixel the minimum to maximum proportions of each material represented by the end-members. The fraction image for muddy water for the Ob'-Irtysh image is displayed in Plate 2a as a color-density slice where the highest proportions of the fraction of muddy water are shown in yellow and red and the lowest proportions of the fraction of muddy water are shown in blue. For the Taquari River image (Plate 2b), fraction images of muddy water, vegetation, and clear water were combined into a color composite of the additive colors of red, green, and blue, respectively. The brightest hues for each color indicate the highest fraction of that end-member material in the pixel. For example, bright red, bright green, and dark blue would produce bright yellow, which could be interpreted as vegetation covered by muddy water. The floodplain of the Altamaha River is forested and does not lend itself readily to examination with optical data during most of the flood season. Therefore the results from the Altamaha River image analysis are shown in black and white and simply show the location of the river channel derived from the muddy water fraction image (Figure 4).

2.2. Field Methods

Field measurements of magnitude and direction of currents and suspended sediment concentrations were collected on the Amazon and Altamaha Rivers prior to and during flooding. Procedures described by *Mertes* [1994] and *Mertes et al.* [1993] involve collection of a bottle sample for suspended sediment that was subsampled for filtering on tared filters with a pore size of 0.45 μm. Velocity measurements were made with a hand-held current meter over 2-min intervals. Field observations, aerial photographs, and aerial videos were also used to produce qualitative maps of water type during floods on the Amazon, Altamaha, and Taquari Rivers.

3. Analysis of Results

3.1. Mississippi and Missouri Rivers

During the summer of 1993 the upper Missouri and Mississippi Rivers flooded for several weeks [*SAST*, 1994] as the result of a wet spring followed by intense midsummer rainstorms [*Gomez et al.*, 1995]. A comparison of the inundation hydrology of these two heavily engineered and managed channel-floodplain systems provides examples of both types of inundation hydrology illustrated in Figure 2. For much of its length, the Missouri River on July 25, 1993, filled its floodplain from valley wall to valley wall with river water. The image in Plate 1a shows river water in the meandering channel with concentrations exceeding 200 mg L^{-1}. The red color of the high concentrations is spread across the floodplain especially on the eastern or downstream end of the river reach in a pattern similar to the one shown in Figure 2a. However, upstream of the most sinuous river bend and north of the eastern end of the river reach are areas containing water with much lower sediment concentrations (<60 mg L^{-1}).

The spatial patterns of mixing of the water types suggest that the clearer waters are not the result of sediment decanting from river water, but they may have been present as the result of ponding on the floodplain surface. In the northeast floodplain area oxbow lakes near Glasgow, Missouri (described in detail by *SAST* [1994]), are filled with nearly clear water. The potential perirheic zone is either masked by vegetation, or the local water resisted the entry of river water and was backed up by the damming effect of the channel flow. At the other end of the reach one can see a small plume of pink (140–160 mg L^{-1}) to yellow (100 mg L^{-1}) water entering the clearer water on the floodplain in the southwestern part of the image.

The cone-shaped entry of water through levee breaks on the Missouri River is mimicked on the Mississippi River, as shown in Plate 1b. In the case of the Mississippi River the suspended sediment concentrations were significantly lower (60–120 mg L^{-1}) than the Missouri River during July 1993. Higher sediment concentrations (80–140 mg L^{-1}) are observed in the core of the Mississippi plumes and generally reflect sediment mobilization in response to local scour at the break site [*Gomez et al.*, 1995]. The spatial pattern of water types for the Mississippi example also suggests that the clear flow at the back edge of the floodplain is present owing to ground saturation and ponding. If the clear water were the result of decanted river water, then the shape of the perirheic zone would presumably conform to the shape of the levee-break plumes rather than appear to be rectangular in shape. The rectangular shape of the clear water (blues and greens) suggests the presence of a topographically lower area that may have filled with groundwater and/or rainwater prior to river water entering the leveed area.

3.2. Amazon River

Analysis of Landsat images showed that the inundation hydrology of the Amazon River varies seasonally [*Mertes et al.*, 1993; *Mertes*, 1994] and spatially [*Mertes et al.*, 1995], confirming modelling results reported by *Richey et al.* [1989]. The central Amazon River is shown in Plate 1c during a very high flood that occurred in the summer of 1989. Most river levees throughout this reach were topped by a minimum of 1.5 m of flow [*Mertes*, 1990], and yet the most striking feature of the image is the narrowness of the band of rainbow-colored sediment-laden river water (60–180 mg L^{-1}) relative to the broad expanses of clear floodplain water in blues (<40 mg L^{-1}). Other images examined for this reach [*Mertes et al.*, 1993; *Mertes*, 1994] and field measurements of sediment concentration and alkalinity throughout the region for floods in 1986 and 1991 [*Mertes*, 1990; L. A. K. Mertes, unpublished data, 1986, 1991] confirm that most of the sediment-rich water is confined to the narrow zone near the river channel and that a perirheic zone of diluted river water covers large areas of the floodplain (compare Plate 1c and Figure 2b). In addition, a simulation of this flood in this reach computed from a two-dimensional hydrodynamic, finite difference model [*Mertes*, 1990, 1994] showed nearly stagnant flow conditions along the back edges of the floodplain that are apparently covered with clear local water, as shown in Plate 1c.

Mertes et al. [1995, 1996] showed that the spatial variation of the perirheic zone along the river is partially a function of the geomorphology. Upstream reaches are characterized by a high density of floodplain channels that confine flooding river water and therefore reduce the potential for mixing of river water with locally derived water during flooding. Middle reaches of the river (Plate 1c) are characterized by nonchannelized overbank flows across levees that result in greater mixing of water types in the more-open floodplain areas. In the downstream reaches, many large lakes have sufficient hydraulic head to prevent river water from entering large sections of the floodplain, not unlike the oxbow lakes of the Missouri River observed in Plate 1a.

The lateral extent of incursion of river water into the floodplain varies from approximately 5 km in the upstream reaches to 5 to 15 km in the reach shown in Plate 1c. Occasionally, incursions as long as 20 km occur as channelized flow into lakes in the downstream reaches. On the basis of chemical and hydrologic data *Forsberg et al.* [1988] and *Lesack and Melack* [1995] also showed that the spatial extent and volume of river water incursion into Amazon lakes depends on the ratio of the local drainage basin area to lake area and distance from the river.

3.3. Ob' and Irtysh Rivers

The complexity of inundation hydrology is apparent across many different types of rivers subjected to extremely different climatic conditions. Floods along rivers of western Siberia occur in the summer after the river ice has melted. One of the largest north flowing river systems is the Ob'-Irtysh River system, shown in Plate 2a. The SPOT image shows was analyzed with spectral mixture analysis to illustrate qualitatively the variation in sediment concentration across the channel-floodplain area. The Irtysh flow (orange) apparently supported higher sediment concentrations than the more northern Ob', while the floodplain wetlands between the two rivers [*Yasuoka et al.*, 1994] appears to be flooded with water of a sediment concentration similar to that carried in the Ob' River. These

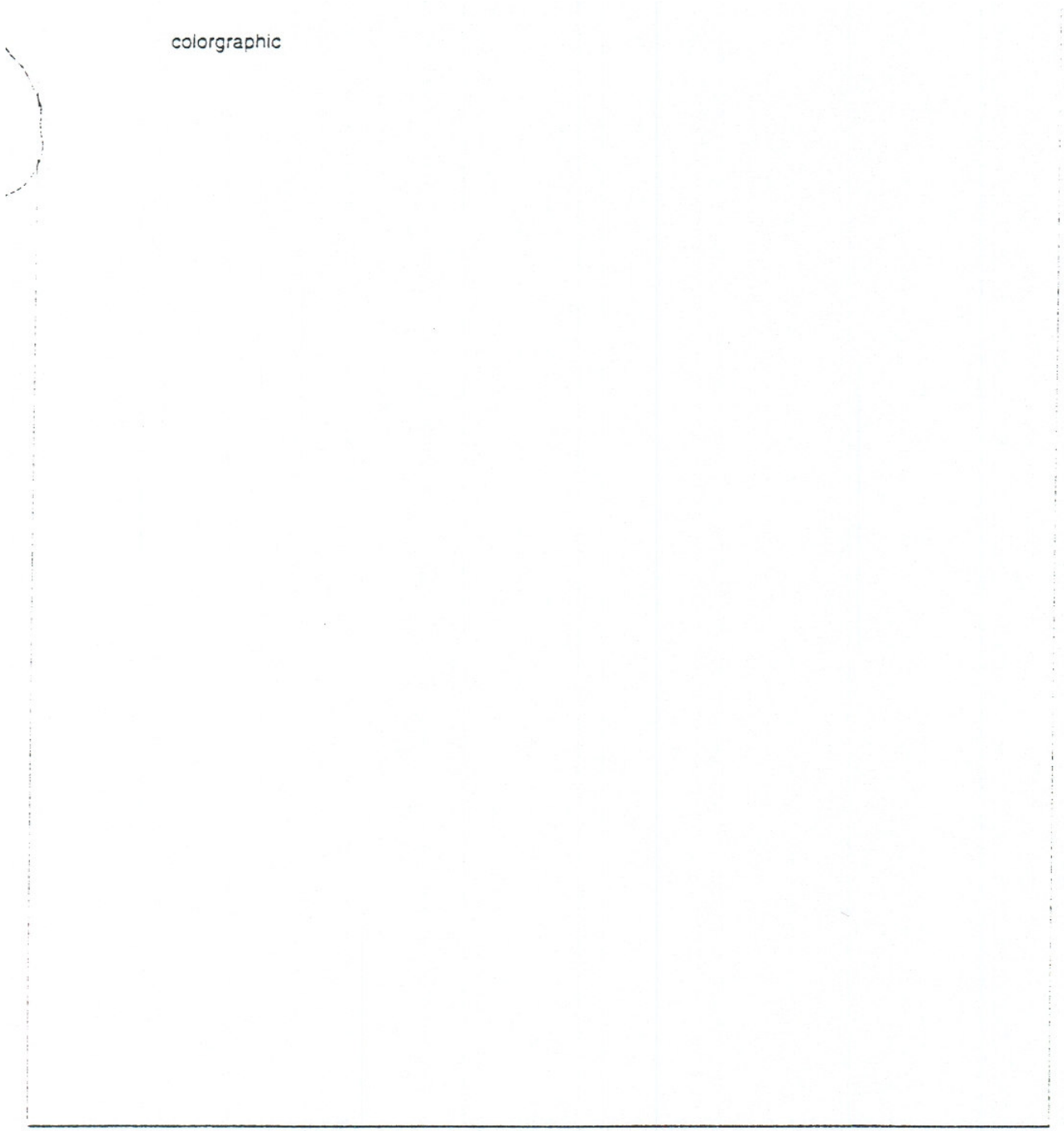

Plate 1. Landsat Thematic Mapper images calibrated for sediment concentration for reaches of three different rivers. For clarity, areas unaffected by flooding or areas where vegetation screened the water surface are masked. Flow direction is from west to east for the Missouri and Amazon, and from north to south for the Mississippi. (a) Missouri River during the summer flood of 1993; (b) Mississippi River during the summer flood of 1993; and (c) Amazon River during the 1989 annual flood.

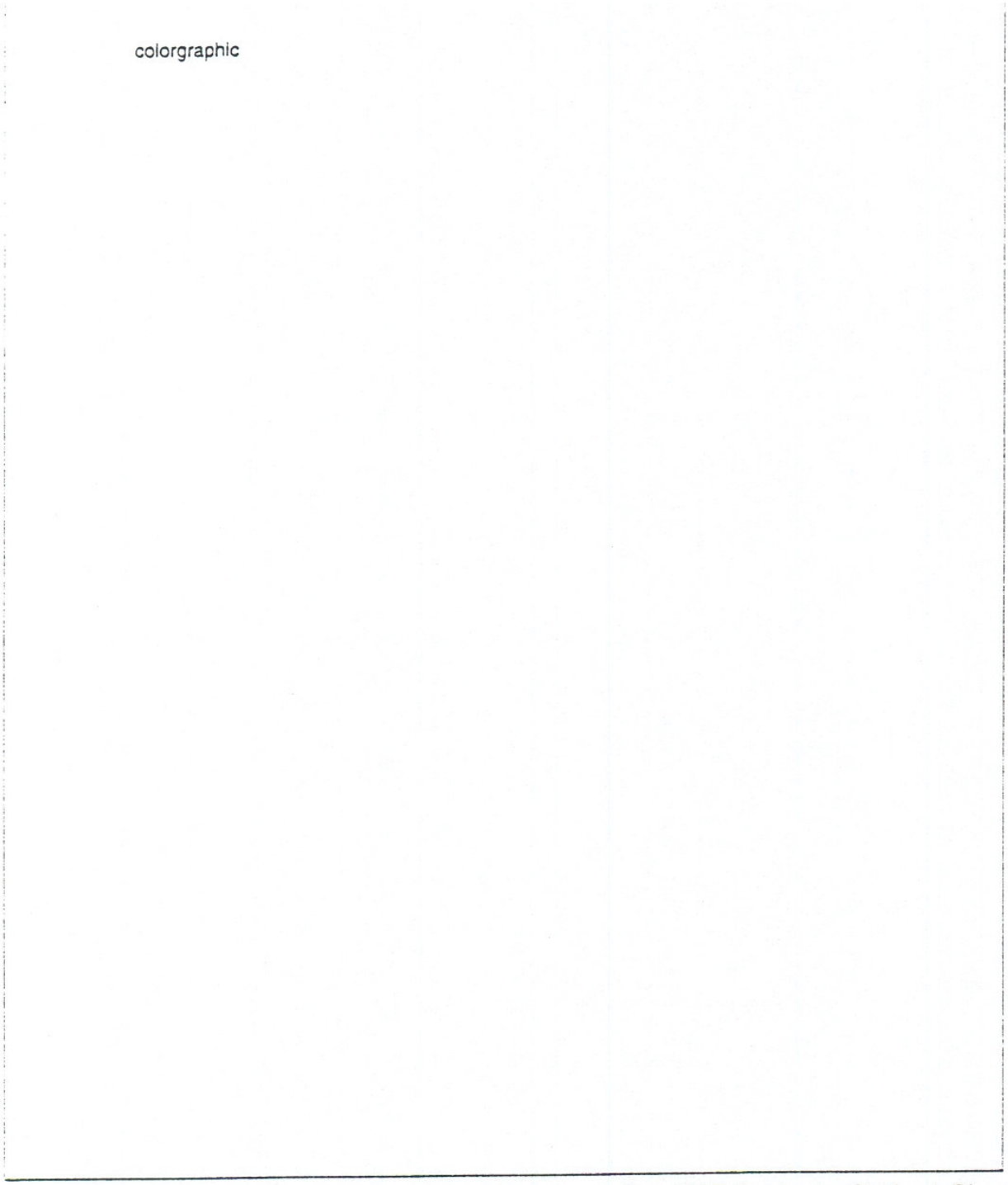

Plate 2. (a) Color-density slice of a muddy water fraction image from SPOT data for the Ob'-Irtysh Rivers showing relative turbidity with low sediment concentrations in blue and increasing concentrations progressing through green and yellow to the highest concentrations, in red. For clarity, areas unaffected by flooding or areas where vegetation screened the water surface are masked. The approximate boundary of the incursion of sediment-rich river water and the perirheic zone is marked by the patterned arrow that points in the flow direction. (b) Landsat Thematic Mapper image processed to fraction data which are rendered as a color composite with muddy water as red, vegetation as green, and clear water as blue. Shallow clear water is magenta and deep clear water is blue. The muddiest water appears as bright red in the meandering Taquari River channel. The approximate boundary of the incursion of sediment-rich river water and the perirheic zone is marked by the patterned arrow that points in the flow direction.

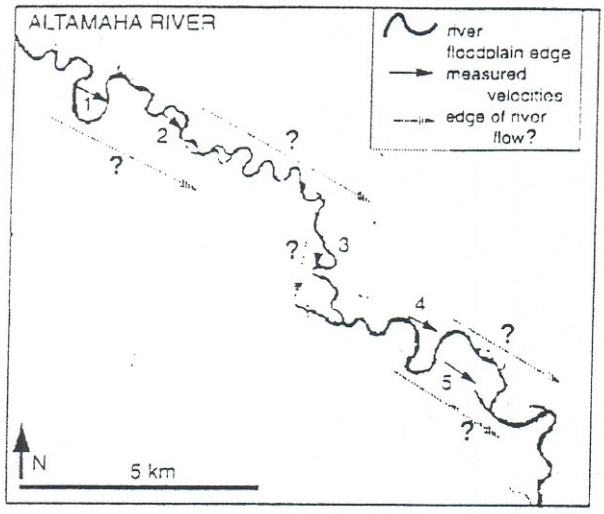

Figure 4. Black and white rendering of muddy water fraction image for the Altamaha River. The approximate boundary of the floodplain was estimated from aerial photographs, remote sensing data, and topographic maps. The solid, numbered arrows mark river bends for which velocity measurements were made during flooding in November 1994 and February 1995. These numbered arrows indicate the direction of flow across the area of the river bends. The range of (surface) and [depth-averaged] velocities in meters per second measured at these river bends include (1) (0.08–0.40), [0.02–0.41]; (2) (0.11–0.24), [0.04–0.12]; (3) (0.05–0.21), [0.00–0.16]; (4) (0.11–1.03), [0.02–0.76]; and (5) (0.06–0.62), [0.03–0.34] over depths ranging from 0.5 to 2 m. Patterned arrows indicate the proposed boundary of the incursion of river water and the perirheic zone.

patterns are confirmed by unpublished field observations and measurements that show that the Ob' usually carries lower sediment concentrations than the Irtysh (R. H. Meade, personal communication, 1997). The region of the perirheic zone is estimated as the patterned arrow, which marks an approximate boundary to river water incursion that is about 5 to 10 km from the river channel. Perhaps the clear water (blue) present at the distal end of the floodplain and in the round lakes in the southwestern corner is ponded water from in situ melting of snow.

3.4. Taquari River

The Taquari River flows through the core of the Pantanal wetlands. Throughout its length, the Taquari River changes from a meandering, single-thread channel that averages approximately 200 m in width to a distributary system covering tens of kilometers of wetlands with channels that range in width from a few meters to 200 m [*Mertes and Souza*, 1995; O. Souza unpublished data, 1996). Plate 2b includes the beginning of the anastomosing section with the Taquari River shown as a bright red conduit of sediment-rich water. Although no stage data are available for this reach of the Taquari for 1988, precipitation totals were above average, and it is known that flooding occurred during this time (O. Souza, personal communication, 1996). In the northeastern corner of the image shown in Figure 5b the river overflowed the southern levee, and sediment-rich water entered the floodplain. The approximate boundary of the incursion of sediment-rich river water is marked by the patterned arrow and increases from less than 1 km near the levee break to over 5 km several kilometers downstream. The red, orange, and yellow zones in this part of the floodplain indicate vegetation covered with mud or muddy water, in contrast to the magenta and blue clear water of the floodplain at greater distances from the river. Examination of the entire Taquari floodplain suggests that for this flood the direct influence of sediment-rich river water extends less than 10 times the width of the corresponding channel. In other words, the direct influence of river water is on the order of 2 to 4 km on either side of the channel inside of a flooded wetland expanse of over 140,000 km^2 [*Mertes and Souza*, 1995].

3.5. Altamaha River

On the basis of field observations this channel-floodplain system is especially susceptible to saturation of the floodplain prior to arrival of the flood wave. In early October 1994 and mid-November 1995, conditions on the floodplain were documented through ground measurements and aerial photography. In both cases the floodplain was nearly completely covered with water carrying essentially no sediment (unpublished data, 1994, 1995) while the river was still rising but was below bankfull level. In particular, locally intense rainfall prior to the crest of the flood also resulted in deep ponding of the floodplain prior to the October 1994 flood and presumably influenced the ability of the river water to enter the floodplain. Several cross sections across the floodplain indicate that patches of ponded water on the floodplain not directly connected to the surface flow of the river during rising water were often decimeters higher or lower in elevation than the river water surface. The relative elevation difference immediately adjusted to zero once the connection to the river was made as higher flows topped intervening barriers. Hence, in some locations on the floodplain when the surface connection to the river flow occurred, the water level increased more than a meter, while the river water surface had risen only a few decimeters.

Overbank flow conditions were sampled during mid-November 1994 and mid-February 1995. Current velocity measurements of flow magnitude and direction show that the river flow typically enters the floodplain at the inflection point of the arc and reenters the river at the downstream end along a relatively direct path with a strong downvalley component (Figure 4). These flow patterns indicate that the extent of the incursion of the river water may be controlled by the bend geometry, because the river flows obliquely across the floodplain in a relatively straight line across the back side of the river bends. Thus the river water may affect only a narrow zone of the floodplain that is on the scale of the amplitude of the largest river bends (Figure 4), which is approximately 2 to 4 km in a floodplain that can reach 20 km in width. All of these data suggest that the combination of bend geometry and barriers to surface connectivity such as levees, appears to control the location of the perirheic zone along the Altamaha River.

4. Discussion

4.1. Spatial and Temporal Variation of the Perirheic Zone

The hyporheic and perirheic zones should vary spatially and temporally along river corridors (Figure 5). Finer alluvium in floodplains will tend to limit the development of a hyporheos and accentuate the development of a perirheos by reducing the

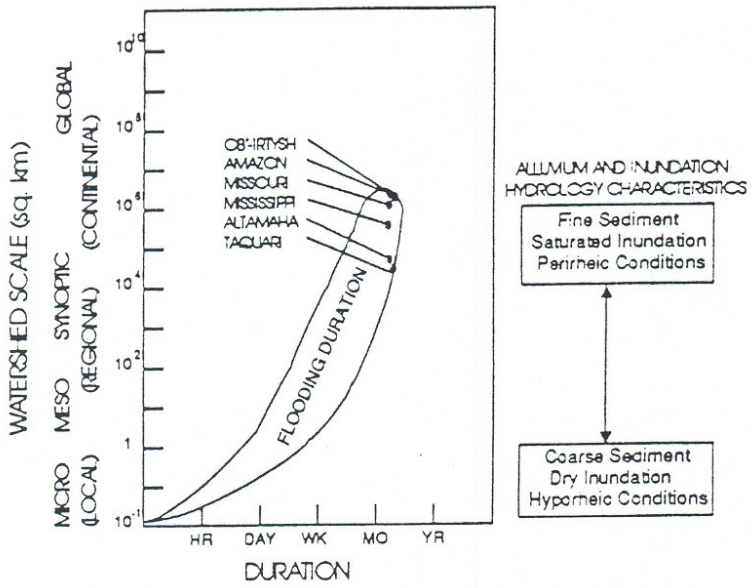

Figure 5. Space-time domain for inundation hydrology and associated floodplain characteristics [after *Hirschboek*, 1988]. The rivers for which data are reported are shown with respect to the scale of the contributing watershed to the main channel at the corresponding gage (see Table 1) and the estimated average duration of annual flood events. The relative scale at the right represents a conceptual framework for considering the relations among alluvium texture (fine versus coarse), inundation hydrology pattern (see Figure 2), and the tendency for hyporheic versus perirheic conditions to dominate during flooding.

rate of flow through the subsurface and increasing the potential for surface ponding. Temporal variation in the spatial patterns of precipitation cells generating runoff for floods will cause variation in the relative arrival times to the floodplain of local versus regional runoff. The differences in timing of the hydrological events will partially vary with the size of the drainage basin and are expected to be most severe in the largest basins where regional storms produce slowly translated flood waves, while locally intense rainfall saturates floodplains.

Flows across floodplain surfaces during inundation were shown to vary in rivers from the Arctic to the Amazon in patterns that reflect their degree of river engineering, geomorphology, and hydroclimatology. The heavily engineered floodplain of the Missouri constrains flows sufficiently so that the river is capable of filling its floodplain with river water during significant floods. The optical data reported here provide new information on the water quality patterns that are complementary to the sedimentation and inundation boundary patterns described by *Izenberg et al.* [1996]. The engineering of the levee districts of the Mississippi River resulted in another distinct pattern of river water incursion, where levee breaks produced scouring plumes of sediment-rich water that dispersed in cone-like shapes across the lakelike environment of the levee interior [*Gomez et al.*, 1995]. Perirheic zones conform to both the shape at the edge of the river flow on the floodplain as well as to geomorphology of the floodplain surface.

The unobstructed flood flows of rivers like the Amazon, Ob'-Irtysh, Taquari, and Altamaha do not immediately result in valley wall to valley wall inundation by river water, partially because of the influence of the geomorphology of the channel-floodplain area. The Altamaha River exemplifies the influence of geomorphic controls on inundation hydrology in that the location and extent of the perirheic zone appears to be a direct function of the bend geometry and distribution of natural obstructions such as levees delineating old channels. Spatial patterns of the perirheic zone along 3000 km of the Amazon also vary with respect to the geomorphology and, especially, lake hydrology [*Mertes et al.*, 1995, 1996; *Forsberg et al.*, 1988; *Lesack and Melack*, 1995]. For example, in the central reach shown in Plate 1c, the diversity of geomorphic landforms, including scroll bars, swales, lake shores, lake deltas, and floodplain drainage channels, is higher than in other reaches probably because the extent and variability of the perirheic zone provides innumerable opportunities for variation in the patterns of erosion and deposition on the floodplain [*Mertes et al.*, 1995, 1996; *Dunne et al.*, 1997].

4.2. Significance of the Perirheic Zone

The perirheic zone may significantly influence the geomorphology, biogeochemistry, productivity, and vegetation cover of floodplains. The geomorphology of the floodplain will be affected primarily by the incursion of sediment-rich river water into the floodplain. For example, *Wilken et al.* [1994] described the significance of flooding area and the spread of contaminated sediments for the Mulde River, Germany (see Figure 3 for location). Loci of deposition, and hence construction of landforms, will be limited to the channel side of the perirheic zone but could shift if the mix of regional and local water available during floods is altered. Scour during extreme floods [*Miller*, 1995; *Bornette et al.*, 1994a] may never be repaired in areas on the floodplain side of the perirheic zone due to a lack of sediment.

The variability in biogeochemistry throughout the perirheic zone is probably considerable, and few studies exist. Extensive field investigations carried out during the Piren-Seine project [*Fustec and Marsily*, 1996] include detailed examination of the

topography of the Seine floodplain and the associated hydrology, biogeochemistry, mineralogy, and texture of the underlying sediments. The Seine River floodplain is heavily managed, yet upstream of Paris, near the Aube River confluence, it is still subjected to annual floods of significant volume. Transects across the floodplain show significant relief (>2 m) [*Dzana and Guillard*, 1996]. The low areas, especially near terrace boundaries, appear to be subjected to saturation by groundwater and local runoff from surrounding slopes (E. Fustec, personal communication, 1996). Nutrient levels measured in well water from points distributed across the floodplain show that the local agricultural drainage, which is high in nutrients, dominates at the edges of the floodplain, while river water with lower nutrient concentrations dominates near the channel. A hyporheic zone of mixing apparently exists between the extremes. Turbidity differences visible from aerial photography recorded during floods show a similar pattern in the surface flows. Nearly half of the floodplain, on the order of 5 to 10 km, is inundated primarily by clear groundwater and apparently never experiences flow directly from the river. Hence the damming of groundwater and locally derived runoff by the river water during inundation creates an extensive perirheic zone in the middle of the floodplain.

Engle and Melack [1993] reported on nutrient and productivity gradients in the seston and periphyton of floating meadows in the perirheic zone of a central Amazon floodplain lake. The transition from still to flowing conditions, combined with increased nutrient supply and turbidity, resulted in a seasonal high for epiphytic algal biomass and a seasonal low for phytoplankton biomass. In experiments, undiluted river water decreased the epiphytic algal biomass, suggesting that mixing of river water with clearer floodplain water is essential for maintaining high levels of productivity.

Bornette et al. [1994b] and *Bornette and Amoros* [1991] described the influence of water mixing on the pattern of vegetation in the Rhône River floodplain (see Figure 3 for location). Bornette and colleagues used principal components and canonical correspondence techniques to analyze field data of vegetation cover, hydrology, and sediment characteristics on sections of the Rhône River floodplain subjected to different river management techniques. They showed that water supplied by groundwater to the floodplain surface had a significant influence on community structure and composition, with species responsive to nutrient-poor water prevalent in zones dominated by groundwater seepage rather than river water. In addition, they showed that seepage flow removed fine sediments and overall reduced the tendency towards infilling of floodplain areas. This effect was especially true in areas no longer subjected to scouring because of the reduction of extreme flood events through river management.

Mertes et al. [1995] used two landscape metrics, percent cover and semivariance, derived from classified remote sensing data to describe the spatial distribution and heterogeneity of wetland classes in geomorphically representative reaches of the Amazon River. The spatial heterogeneity of the vegetation communities on similar landforms was similar and was greatest where the landforms were most diverse. Landforms were the most diverse where the perirheic zone was extensive, especially in the middle reaches of the river (Plate 1c), which exemplifies the subparallel banding pattern of the perirheos depicted in Figure 2b.

5. Summary

Current models of inundation hydrology rely on the flood pulse concept [*Junk et al.*, 1989], which implies that rivers flood relatively dry floodplains. In this paper, additional patterns of inundation hydrology based on water quality patterns are documented on the basis of field and remote sensing data. Optical remote sensing data provide a critical tool for distinguishing water types and determining the extent of surficial mixing of water types on inundated floodplains because it is possible to determine absolute and relative surface suspended sediment concentrations. The patterns documented for six large rivers show that surficial ponding of water derived from the hyporheos, groundwater saturation, direct rainfall onto the floodplain, melting of snow and ice, runoff from surrounding slopes, and/or flooding of local tributaries may occur prior to the crest of the floodwave and the onset of overbank flooding from the river channel.

The longitudinal zone resulting from surficial lateral gradients in turbidity and water chemistry on a floodplain includes the elements requisite for an ecotone, in that it derives resources from multiple "homogeneous" patches and provides a temporally and spatially dynamic boundary between these resource patches. With reference to the hyporheos, this surface zone of mixing at the edge of the flowing river water on inundated floodplains is named the "perirheic zone." As documented in this paper, the floodplains of large rivers from the Arctic to the Amazon are only partially inundated with river water during floods and thus contain extensive perirheic zones.

On the basis of these observations, inundation hydrology depends on the geomorphology of the channel-floodplain area, especially with regard to alluvium texture; bend geometry; meander train width, valley width, and the presence of natural or constructed barriers on the floodplain; and the relative contributions of local and regional water, which are in turn a function of the hydroclimatology. For example, depending on the temporal and spatial patterns of the hydroclimatology, intense local rainfall prior to the flood crest may produce enough flow to prevent the entry of river water onto a floodplain surface. Simulations of this dynamic mixing must account for the magnitudes and composition of all water sources, the magnitude and direction of exchange of water between the channel and floodplain, and the lateral and longitudinal pressure gradients across the water surfaces. Combining two-dimensional hydrodynamic models with appropriate compositional inputs from contributing flows [*Mertes*, 1990, 1994] is a promising technique for quantitative analysis of the dynamics of the perirheic zone in different rivers. Through these types of modelling efforts, it will be possible to quantify the influence of the perirheic zone on the geomorphology, biogeochemistry, productivity, and vegetation cover of floodplains.

Acknowledgments. This research was supported by funds from NSF, NASA, and the Japanese Society for Promotion of Science. The Amazon image was obtained from R. Almeida Filho of the Instituto Nacional Pesquisas Especiais of Brazil (INPE). T. Krug of INPE supplied the image of the Taquari River, and O. Souza helped with image processing. The Mississippi and Missouri images were provided by B. Gomez. The Ob'-Irtysh River image analysis was developed in collaboration with Y. Yasuoka and M. Tamura of the National Institute for Environmental Studies of Japan. L. Smith provided the discharge data for the Ob'-Irtysh River. Comments from V. Baker, E. Safran, K. Seeley, and two anonymous reviewers helped improve the final manuscript. Discussions with S. Cooper, O. Sarneile, N. Barbee, K. Klose, and S. Diehl contributed to coining of the word "perirheic." Camrex contribution number 85.

References

Bencala, K., A perspective on stream-catchment connections, *J. N. Am. Benthol. Soc.*, *12*, 44–47, 1993.

Bobrovitskaya, N. N., C. Zubkova, and R. H. Meade, Discharges and yields of suspended sediment in the Ob' and Yenisey Rivers of Siberia, *LAHS Publ. 236*, 115–123, 1996.

Bornette, G., and C. Amoros, Aquatic vegetation and hydrology of a braided river floodplain, *J. Veg. Science*, *2*, 497–512, 1991.

Bornette, G., C. Amoros, and D. Chessel, Effect of allogenic processes on successional rates in former river channels, *J. Veg. Sci.*, *5*, 237–246, 1994a.

Bornette, G., C. Amoros, and G. Collilieux, Role of seepage supply in aquatic vegetation dynamics in former river channels: Prediction testing using a hydroelectric construction, *Environ. Manage.*, *18*, 223–234, 1994b.

Castro, N. M., and G. M. Hornberger, Surface-subsurface water interactions in an alluviated mountain stream channel, *Water Resour. Res.*, *27*, 1613–1621, 1991.

Dahm, C. N., and H. M. Valett, Hyporheic zones, in *Methods in Stream Ecology*, edited by F. R. Hauer and G. A. Lamberti, pp. 107–119, Academic, San Diego, Calif., 1996.

Dekker, A. G., T. J. Malthus, and H. J. Hoogenboom, The remote sensing of inland water quality, in *Advances in Environmental Remote Sensing*, edited by F. M. Danson and S. E. Plummer, pp. 123–142, John Wiley, New York, 1995.

Dynesius, M., and C. Nilsson, Fragmentation and flow regulation of river systems in the northern third of the world, *Science*, *266*, 753–762, 1994.

Dunne, T., L. A. K. Mertes, R. H. Meade, J. E. Richey, and B. R. Forsberg, Sediment budget of the Amazon River, *Geol. Soc. Am. Bull.*, in press, 1997.

Dzana, J.-G., and S. Gaillard, Zones inondables et topographie des lits majeurs: L'exemple de l'Aube et de la Seine supériuere, *Ann. Geogr.*, *79*, 191–200, 1996.

Dzana, J.-G., S. Gaillard, J.-M. Grisony, A. Guffroy, and R. Mussot, Etude des plaines d'inondation et de l'expansion des crues dans les fonds de vallées de la Seine supérieure et de l'Aube, in *Corridor fluvial—Piren-Seine 1995 Report*, chap. 2, edited by E. Fustec and B. Marsily, Lab. de Géol. Appl., Univ. Pierre et Marie Curie, Paris, 1996.

Engle, D. L., and J. M. Melack, Consequences of riverine flooding for seston and the periphyton of floating meadows in an Amazon floodplain lake, *Limnol. Oceanogr.*, *38*, 1500–1520, 1993.

Forsberg, B. R., A. H. Devol, J. E. Richey, L. A. Martinelli, and H. dos Santos, Factors controlling nutrient concentrations in Amazon floodplain lakes, *Limnol. Oceanogr.*, *33*, 41–56, 1988.

Fustec, E., and G. Marsily (Eds.), *Corridor fluvial—Piren-Seine 1995 Report*, Lab. de Géol. Appl., Univ. Pierre et Marie Curie, Paris, 1996.

Gomez, B., L. A. K. Mertes, J. D. Phillips, F. J. Maglilligan, and L. A. James, Sediment characteristics of an extreme flood: 1993 upper Mississippi River valley, *Geology*, *23*, 963–966, 1995.

Hakenkamp, C. C., H. M. Valett, and A. J. Boulton, Perspectives on the hyporheic zone: Integrating hydrology and biology: Concluding remarks, *J. N. Am. Benthol. Soc.*, *12*, 94–99, 1993.

Hayden, B. P., Flood climates, in *Flood Geomorphology*, edited by V. R. Baker, R. C. Kochel, and P. C. Patton, pp. 13–26, John Wiley, New York, 1988.

Heiler, G., T. Hein, F. Schiemer, and G. Bornette, Hydrological connectivity and flood puses as the central aspects for the integrity of a river-floodplain system, *Reg. Rivers Res. Manage.*, *11*, 351–361, 1995.

Hendricks, S. P., Microbial ecology of the hyporheic zone: A perspective integrating hydrology and biology, *J. N. Am. Benthol. Soc.*, *12*, 70–78, 1993.

Hirschboeck, K. K., Flood hydroclimatology, in *Flood Geomorphology*, edited by V. R. Baker, R. C. Kochel, and P. C. Patton, pp. 27–49, John Wiley, New York, 1988.

Hoiland, M. M., Wetlands and environmental gradients, in *Wetlands: Environmental Gradients, Boundaries, and Buffers*, edited by G. Mulamoottil, B. G. Warner, and E. A. McBean, pp. 19–43, Lewis Publ., New York, 1996.

Hughes, D. A., Flooding and floodplain inundation, Ph.D. dissertation, 252 pp., Univ. Coll. of Wales, Aberystwyth, 1978.

Hughes, D. A., Floodplain inundation: Processes and relationships with channel discharge, *Earth Surf. Process*, *5*, 297–304, 1980.

Izenberg, N. R., R. E. Arvidson, R. A. Brackett, S. S. Saatchi, G. R. Osborn, and J. Dohrenwend, Erosional and depositional patterns associated with the 1993 Missouri River floods inferred from SIR-C and TOPSAR radar data, *J. Geophys. Res.*, *101*, 23,149–23,167, 1996.

Junk, W. J., P. B. Bayley, and R. E. Sparks, The flood pulse concept in river-floodplain systems, in *Proceedings of the International Large River Symposium*, edited by D. P. Doge, pp. 110–127, *Can. Fish. Aquat. Sci. Spec. Publ.*, 1989.

Kirk, J. T. O., *Light and Photosynthesis in Aquatic Ecosystems*, 401 pp., Cambridge Univ. Press, Cambridge, 1986.

Lesack, L. F. W., and J. M. Melack, Flooding hydrology and mixture dynamics of lake water derived from multiple sources in an Amazon floodplain lake, *Water Resour. Res.*, *31*, 329–346, 1995.

Lewin, J., and D. A. Hughes, Welsh floodplain studies, II, Application of a qualitative inundation model, *J. Hydrol.*, *46*, 35–49, 1980.

Markham, B. L., and J. L. Barker, Landsat MSS and TM post-calibration dynamic rantes, exoatmospheric and at-satellite temperatures, *EOSAT Landsat Tech. Notes*, Aug., 3–5, 1986.

Mertes, L. A. K., Hydrology, hydraulics, sediment transport, and geomorphology of the central Amazon floodplain, Ph.D. dissertation, 225 pp., Univ. of Wash., Seattle, 1990.

Mertes, L. A. K., Rates of flood-plain sedimentation on the central Amazon River, *Geology*, *22*, 171–174, 1994.

Mertes, L. A. K., and O. S. Souza, Classification of the Pantanal wetlands during high water based on spectral mixture analysis of Landsat Thematic Mapper data, paper presented at Application of Remote Sensing to the Study of the Pantanal, Corumbá, Brazil, Oct. 9–12, 1995.

Mertes, L. A. K., M. O. Smith, and J. B. Adams, Estimating suspended sediment concentrations in surface waters of the Amazon River wetlands from Landsat images, *Remote Sens. Environ.*, *43*, 281–301, 1993.

Mertes, L. A. K., D. L. Daniel, J. M. Melack, B. Nelson, L. A. Martinelli, and B. R. Forsberg, Spatial patterns of hydrology, geomorphology, and vegetation on the floodplain of the Amazon River in Brazil from a remote sensing perspective, *Geomorphology*, *13*, 215–232, 1995.

Mertes, L. A. K., T. Dunne, and L. A. Martinelli, Channel-floodplain geomorphology along the Solimões-Amazon River, Brazil, *Geol. Soc. Am. Bull.*, *108*(9), 1089–1107, 1996.

Miller, A. J., Valley morphology and boundary conditions influencing spatial patterns of flood flow, in *Natural and Anthropogenic Influences in Fluvial Geomorphology: The Wolman Volume*, *Geophys. Monogr. Ser.*, vol. 89, edited by J. E. Costa et al., pp. 57–81, AGU, Washington, D. C., 1995.

Naiman, R. J., H. Décamps, J. Pastor, and C. A. Jonston, The potential importance of boundaries to fluvial ecosystems, *J. N. Am. Benthol. Soc.*, *7*, 289–306, 1988.

Orghidan, T., Ein neuer Lebensraum des unterirdischen Wassers, der hyporheische Biotop, *Arch. Hydrobiol.*, *55*, 392–414, 1959.

Palmer, M. A., Experimentation in the hyporheic zone: challenges and perspectives, *J. N. Am. Benthol. Soc.*, *12*, 84–93, 1993.

Richey, J. E., L. A. K. Mertes, T. Dunne, R. Victoria, B. R. Forsberg, A. Tancredi, and E. Oliveira, Sources and routing of the Amazon River flood wave, *Global Biogeochem. Cycles*, *3*, 191–204, 1989.

Scientific Assessment and Strategy Team, Science for floodplain management into the 21st century: A blueprint for change, Part V, Report of the Interagency Floodplain Management Review Committee, 272 pp., Washington, D. C., 1994.

Smith, M. O., S. L. Ustin, J. B. Adams, and A. R. Gillespie, Vegetation in deserts, I, A regional measure of abundance from multispectral images, *Remote Sens. Environ.*, *31*, 1–26, 1990.

Stanford, J. A., and J. V. Ward, The hyporheic habitat of river ecosystems, *Nature*, *225*, 64–66, 1988.

Stanford, J. A., and J. V. Ward, An ecosystem perspective of alluvial rivers: Connectivity and the hyporheic corridor, *J. N. Am. Benthol. Soc.*, *12*, 48–60, 1993.

Triska, F. J., V. C. Kennedy, R. J. Avanzino, G. W. Zellweger, and K. E. Bencala, Retention and transport of nutrients in a third-order stream in northwestern California: Hyporheic processes, *Ecology*, *70*, 1893–1905, 1989.

U.S. Geological Survey, *Water Data Rep. GA-95-1*, p. 185, 19

Valett, H. M., C. C. Hakenkamp, A. J. Boulton, Perspectives on the hyporheic zone: Integrating hydrology and biology: Introduction, *J. N. Am. Benthol. Soc.*, *12*, 40–43, 1993.

Ward, J. V., and J. A. Stanford, Ecological connectivity in alluvial river

ecosystems and its disruption by flow regulation, *Reg. Rivers Res. Manage.*, *11*, 105–119, 1995.

White, D. S., Perspectives on defining and delineating hyporheic zones, *J. N. Am. Benthol. Soc.*, *12*, 61–69, 1993.

Wilken, M., F. Walkow, E. Jager, and B. Zeschmar-Lahl, Flooding area and sediment contamination of the river Mulde (Germany) with PCDD/F and other organic pollutants, *Chemosphere*, *29*, 2237–2252, 1994.

Witte, W. G., C. H. Whitlock, J. W. Usry, W. D. Morris, and E. Gurganus, Laboratory measurements of physical, chemical, and optical characteristics of Lake Chicot sediment waters, *NASA Tech. Pap. 1941*, 27 pp., 1981.

Yasuoka, Y., M. Tamura, and Y. Yamagata, Application of remote sensing to environmental monitoring—global wetland monitoring, in *Optical Methods in Biomedical and Environmental Sciences*, edited by H. Ohzu and S. Komatsu, pp. 269–272, Elsevier Sci., New York, 1994.

L. A. K. Mertes, Department of Geography and Institute for Computational Earth System Science, University of California, Santa Barbara, CA 93106-4060. (e-mail: leal@geog.ucsb.edu)

(Received August 26, 1996; revised January 24, 1997; accepted February 27, 1997.)